J. Fluid Mech. (1983), *vol.* 126, *pp.* 13–26
Printed in Great Britain

Homeotropic nematics heated from above under magnetic fields: convective thresholds and geometry

By J. SALAN† AND E. GUYON‡
E.S.P.C.I., 10 rue Vauquelin, 75005 Paris, France

(Received 29 January 1982)

The thermal convective instability of a nematic layer aligned perpendicular to horizontal plates displays original characteristics, due to the coupling of the nematic distortion with the temperature gradient; in particular the adverse temperature gradient threshold ΔT_c can be modified by the application of a vertical (stabilizing) or horizontal (destabilizing) magnetic field. In addition, the application of a magnetic field H controls both the threshold of this instability and the geometric form of the instabilities above ΔT_c.

1. Introduction

The study of thermal convective instabilities in nematic liquid crystals has attracted interest over the last 10 years because of their unique characteristics; namely threshold values very different from those in the corresponding Rayleigh–Bénard (RB) instabilities of isotropic materials having similar average characteristics: instabilities under *adverse* temperature gradients (heating from above), control of thresholds and convective geometry by external electric or magnetic fields, and overstable and inverted bifurcation in a geometry complementary to that discussed in the present paper.

In uniaxial nematics, the orientation of the average molecular axis is defined by a director field $\mathbf{n}(\mathbf{r})$ ($|\mathbf{n}(\mathbf{r})| = 1$). Uniform alignment between parallel plates ($\perp$ to z) can be obtained by surface treatment of the inner faces of the cell. *Planar* ($\mathbf{n} \perp z$) and *homeotropic* ($\mathbf{n} \parallel z$) configurations can be produced. The mechanism underlying the original properties of the linear instability modes is the following coupling (figure 1): a director fluctuation $\delta\mathbf{n}(\mathbf{r})$ induces a temperature fluctuation $\theta(\mathbf{r})$ via a heat-focusing effect due to the anisotropy of the thermal diffusivity of the nematic ($\kappa_\parallel/\kappa_\perp \approx 1{\cdot}3$, where $\parallel$ and $\perp$ refer to directions of the heat flux with respect to $\mathbf{n}$ (Vilanove *et al.* 1974); buoyancy forces and convective flow occur under the influence of the modification of the density $\rho(T)$ ($\alpha = (-1/\rho)(\partial\rho/\partial T) > 0$); distortion of the director is induced by the shear gradients (the viscous coefficients α_2 and α_3 of the Leslie stress tensor, which control this coupling, are defined in the appendix). With certain combinations of signs of the coupling terms, the initial director fluctuation is reinforced by the above loop. The characteristic of the linear convective RB instability is strongly modified by the inclusion of the director fluctuation in the instability loop because the time constant t_0 for the diffusive relaxation of the director fluctuation is long compared with those for the relaxation of heat and vorticity, t_t and t_v:

$$t_{0,t,v} = (D_{0,t,v}\, q^2)^{-1}; \quad t_0 \gg t_t \gg t_v. \tag{1}$$

† Permanent address: Departemento de Física Fundamental, U.N.E.D., Apdo Correos 54487 Madrid 3, Spain.

‡ Also at: Laboratoire de Physique des Solides, Université Paris-Sud, 91405 Orsay.

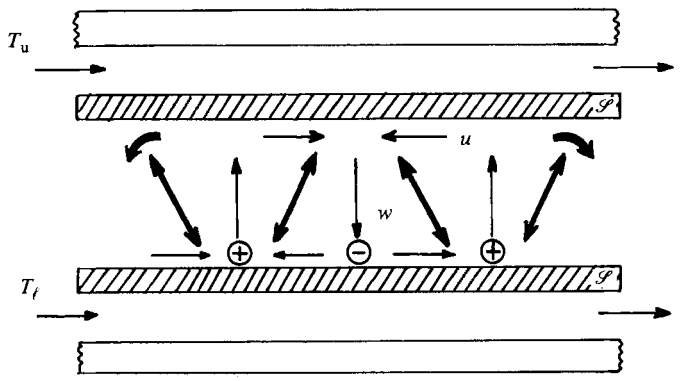

FIGURE 1. Schematic representation of the convective cell emphasizing the coupling leading to instability for an adverse temperature difference $\Delta T = T_\ell - T_u < 0$. The fluctuation of the director $\delta\mathbf{n}(\mathbf{r})$ is represented by the tilting of the double-arrow line; the temperature fluctuation $\theta(\mathbf{r})$ induced by 'heat focusing' is given by $\oplus$ and $\ominus$; buoyancy leads to the velocity field $(u(\mathbf{r}), 0, w(\mathbf{r}))$. The torque on the director created by the field is shown by curved arrows.

$q \approx \pi/d$ is the wavevector of the fluctuation in the plane of the cell, $D_t = \kappa$ is the heat diffusivity, $D_v = \eta/\rho$ is a kinematic viscosity term, $D_0 = K/\gamma$ is a diffusivity for the director orientation (K is a Frank elasticity for the orientation of $\mathbf{n}$, and γ is a viscosity for its relaxation).

The analysis has been developed theoretically for several configurations of $\mathbf{n}$ and ∇T, and has led to predictions and experimental studies of:

(i) Roll instabilities in planar nematics *heated from below* with a threshold 5×10^2 smaller than in the RB isotropic case (Dubois-Violette 1971; Dubois-Violette, Guyon & Pieranski 1974).

(ii) Two-dimensional (square) instability for homeotropic nematics *heated from above* with thresholds comparable to the planar case (Pieranski, Dubois-Violette & Guyon 1973).

(iii) Oscillating instabilities for homeotropic nematics *heated from below* with isotropic-like values of threshold (Lekkerkerker 1977; Guyon, Pieranski & Salan 1979). In this problem, the stabilizing role of the director fluctuations is suppressed by the existence of an oscillation at a frequency $\sim t_t^{-1}$ ($\gg t_0^{-1}$; the velocity relaxes faster than heat in nematics ($t_t \gg t_v$) and follows $\theta(\mathbf{r})$). However the application of a magnetic field along (+) (at right-angles (−)) the orientation at rest leads to a decrease (increase) of t_0 given by

$$t_{0\pm}^{-1}(H) = \frac{Kq^2 \pm \chi_a H^2}{\gamma_1} = \frac{Kq^2}{\gamma_1}\left[1 \pm \left(\frac{H}{H_c}\right)^2\right], \tag{2}$$

and leads in particular to a qualitative change of the nature of the instability when $t_0^{-1}(H) > t_t^{-1}$ (Guyon *et al.* 1979).

In (2) the divergence of t_0 for a large-enough field

$$H_c = \left(\frac{Kq^2}{\chi_a}\right)^{\frac{1}{2}} \tag{3}$$

corresponds to the Freedericksz–Zocher (FZ) homogeneous instability of nematics under external fields (Deuling 1978); χ_a (> 0) is the anisotropic part of the susceptibility leading to alignment of nematics along $\mathbf{H}$. Thus magnetic fields can control the threshold value, the instability mechanism, and the geometry of the instability pattern, which depends on $\mathbf{n}$.

The present article is a detailed study of such effects for homeotropic nematics heated from above (ii). The case of homeotropic materials heated from below (iii) was discussed by Guyon *et al.* (1979, hereinafter referred to as I).

2. Experimental

The experimental set-up was described in I. The inner faces of the transparent sapphire circular disks forming the walls of the horizontal cell (S on figure 1) have been coated with lecithin, which ensures homeotropic alignment of the nematic held between the disks. The material used is MBBA (methoxybenzylidene *p*-(*n*-butyl)aniline), which is nematic between 19 and 45 °C. Homogeneity of orientation is controlled by observing the homogeneity of the dark field across the cell between crossed polarizers. The cell is closed sideways by an insulating Teflon disk of inner diameter $L = 52$ mm, which also serves as a spacer. For the thicknesses used, $d = 0{\cdot}7$, 1 mm, the aspect ratio L/d larger than 50 insures a good regularity of the convective structures in the central part of the cell. Water is circulated at two different temperatures T_ℓ, T_u on the outer faces of the disk and keeps the temperature difference $\Delta T = T_\ell - T_u$ (< 0) stabilized within 0·1°. ΔT is read by a differential thermocouple whose ends are next to the outer faces. The temperature drop across the disks is estimated to be less than 3 % of the total ΔT. The cell is surrounded with a coil of vertical axis and a horizontal-axis pair of Helmholtz coils, which provide magnetic fields up to 400 G of arbitrary direction. The value of the FZ critical field (3), $H_c \approx 120$, 80 G for $d = 0{\cdot}7$, 1 mm, gives a natural scale for the aligning fields ($h = H/H_c$). However, it is not determined accurately in such thick cells, and we will rather use a scaling field H_0 ($\sim H_c$) defined in §3.

The detection of convection makes use of the large birefringence that accompanies the periodic distortion of $\mathbf{n}$ above threshold ΔT_c. The temperature difference is changed by increasing T_u by 0·1 °C steps, keeping $T_\ell = 20$ °C fixed. The time between steps is of several hours around threshold. Typically the growth time for the instability is measured by the larger value: $t_0|1 - \Delta T/\Delta T_c|^{-1}$, where t_0 is the relaxation time for the director (1); $t_0 \sim 10^3$ s for $d = 0{\cdot}7$ mm) and where the temperature-dependent factor shows a 'critical slowing-down' effect associated with the direct birfurcation of the instability problem. In all the experiments reported, we have found no hysteresis in the value of the lowest instability threshold when increasing or decreasing ΔT, within the 0·1 °C accuracy of the experiments. It should be noted, however, that, even in such cases where an inverse bifurcation is expected, as in the Bénard–Marangoni (BM) experiment in isotropic fluids, hysteresis can be quite small and more easily detected from the value of the amplitude of the instability (Gerbaud 1980).

Direct study of the geometry is made from photographs of the pattern or from ciné pictures recorded at low speed (1 image/s).

3. Theoretical predictions

The different situations in thermal convective problems presented in §1 correspond to linear instability modes and can be solved using linearized solutions of the nematohydrodynamic equations found by Ericksen (1962) and Leslie (1968), which describe the coupling between the velocity field $\mathbf{v}(x, y, z, t)$ and the nematic director $\mathbf{n}(x, y, z, t)$. These equations lead to the construction of appropriate forms for the Navier–Stokes equation, for the balance of the torques acting on $\mathbf{n}$, and for the

heat-conduction equation, which, together with the continuity equation $\nabla \mathbf{v} = 0$, completely determine $\mathbf{n}$, $\mathbf{v} = (u, v, w)$, the local pressure p and the local temperature fluctuation θ.

The problem of thermal instabilities in nematic liquid crystals has been treated in several instances after the initial approach of Dubois-Violette (1971) for a planar nematic heated from below. This work used a one-dimensional solution retaining only the effect of the vertical velocity component w and the dependences on the horizontal coordinate x. The effect of thickness is introduced by putting a value for the wavevector $q_x = \pi/d$. Such a simple approach provides an excellent description of the linear instability, consisting of parallel rolls perpendicular to x, and a reasonably good quantitative estimate for the threshold. This approach cannot be extended as such in the present problem sketched in figure 1: the torque acting on the director and due to the gradient component $\partial w/\partial x$ is stabilizing in most nematics (and in particular in MBBA) when a Leslie viscous coefficient α_3 is negative. On the contrary, the gradient component $\partial u/\partial z$ gives a contribution proportional to the Leslie coefficient α_2 ($|\alpha_2| \gg |\alpha_3|$), in the direction of the curved arrow on the figure, which is the dominant torque. The distortion is such that it induces a heat-focusing effect that reinforces the initial velocity fluctuation in the 'instability loop' presented in I. Thus the essential features of the nematic instability, coming from a gradient term $\partial/\partial z$, has to be described through a two-dimensional model. In addition to the approximate solution given in the initial report on the instability by Pieranski *et al.* (1973), Dubois-Violette (1974) gave an exact numerical solution for both planar and homeotropic cases in quantitative agreement with experiment (threshold and wavevector at threshold) (also see Currie 1973).

Barratt & Sloan (1976) also used the continuum theory of nematics to obtain an exact expression for determining the threshold in the two experimental situations. Their analysis agrees with the previous ones and also includes the effect of field along or at right angles with the unperturbed director. The problem was reconsidered by Gabay (1981), who produced numerical results for the effect of a magnetic field on threshold and wavevector in connection with the present experiments.

In the dimensionless parameters introduced by Barratt & Sloan, the field H only enters in combinations of the form $|Kq_x^2 \pm \chi_a H^2|$ for H perpendicular $(-)$ or parallel $(+)$ to $\mathbf{n}$, which, divided by the torque viscosity, gives the form of the natural relaxation rate of the director $\tau_0^{-1}(H)$.

In Gabay's (1981) work, an effective elastic constant $K(q_x)$ is introduced such that

$$K(q_x)\, q_x^2 = K_1 q_x^2 + K_3\left(\frac{\pi^2}{d^2}\right) \pm \chi_a H^2, \tag{4}$$

which expresses the addition of the effect of splay elasticity K_1 of the director along x and the bend elasticity K_3 across the thickness of the film d. The Freedericksz limit is obtained as a softening of the elasticity ($K(q_x) \to 0$) in the presence of a destabilizing field $(-)$ for a critical field

$$H_{c3} = \frac{\pi}{d}\left(\frac{K_3}{\chi_a}\right)^{\frac{1}{2}} \tag{5}$$

and a homogeneous distortion $q_x = 0$. In this limit $\Delta T_c(H_{c3}) = 0$.

On the other hand for small fields ($H \ll H_{c3}$), the value of the threshold $\Delta T_c(H)$ can be obtained from that in zero field $\Delta T_c(0)$ by using a simple analysis in terms of the time constants as done in particular by Guyon & Pieranski (1973). As the orientation is the slow relaxing variable, we expect ΔT_c to vary at t_0^{-1}, where t_0 is obtained from

an expression analogous to (1):

$$t_0^{-1} = \frac{K(q_x)\, q_x^2}{\gamma_1}.$$

This leads to

$$\Delta T_c(H) = \Delta T_c(0)\left[1 \pm \frac{H^2}{H_0^2}\right], \tag{6}$$

with

$$\frac{H_0^2}{H_{c3}^2} = \left[1 + \frac{K_1}{K_3}\frac{q_x^2 d^2}{\pi^2}\right]. \tag{7}$$

The decrease of $\Delta T_c(H)$ due to a destablizing horizontal field has been calculated by Gabay (1981), and is given in figure 2. It clearly shows the difference between H_0,

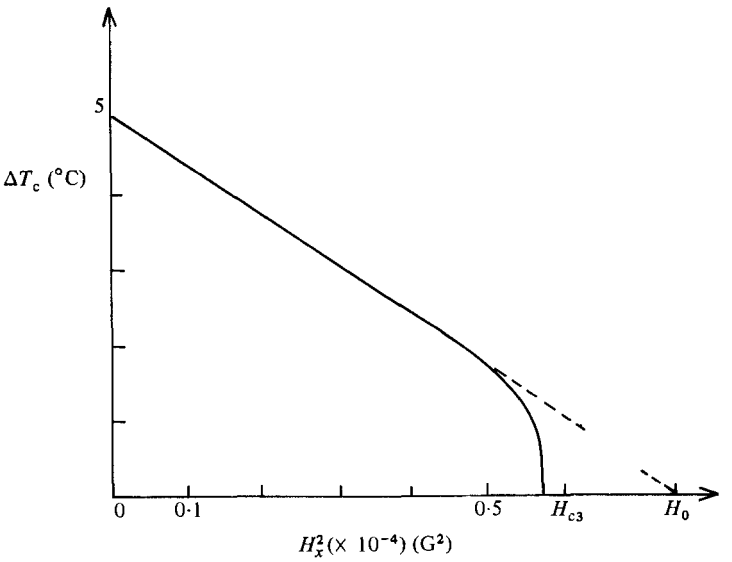

FIGURE 2. Variation of threshold with horizontal magnetic field H_x (theory). The calculation was made with the parameters of MBBA for a film thickness $d = 1$ mm.

which includes both splay and bend distortions near threshold, and the homogeneous limit $H = H_{c3}$. Owing to the different weight given to the factors K_1 and K_3 for different values of fields, it is not possible to obtain a dimensionless form of the $\Delta T_c(H)$ field. The rapid variation of $\Delta T_c(H)$ near H_{c3} is closely connected with that of the reduced wavevector $q_x d/\pi$ near the threshold of the Freedericksz transition given in figure 3.

On the other hand, in a stabilizing field (H along **n**) the increase of wave vector $q_x d/\pi$ with field, as the threshold $\Delta T_c(H)$ increases, is more limited, as indicated from the result of figure 4.

4. Convective thresholds and geometry

In this section, we describe the experimental results at and near the lowest instability threshold for various magnetic-field situations and for two different thicknesses $d = 0{\cdot}7$, 1 mm.

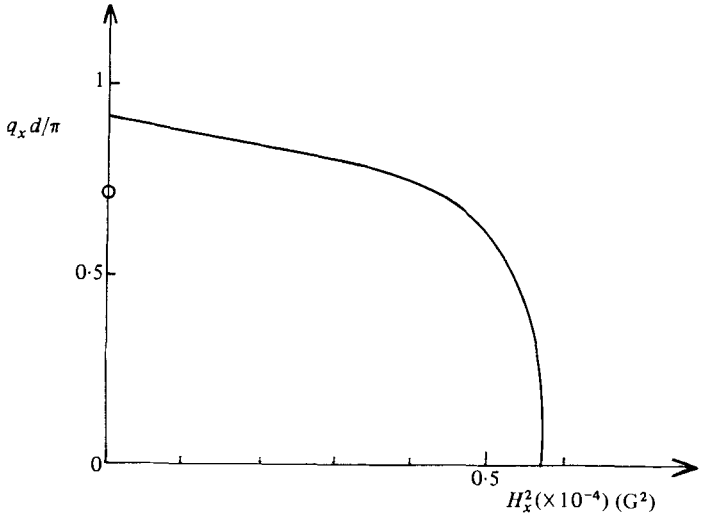

FIGURE 3. Corresponding variation of the horizontal wavevector of the roll structure (for $H_x = 0$ the structure is made of squares; for $\Delta T_c = 0$ it is the homogeneous FZ instability). (The calculations of figure 2, 3 and 4 have been made by Gabay (1981).)

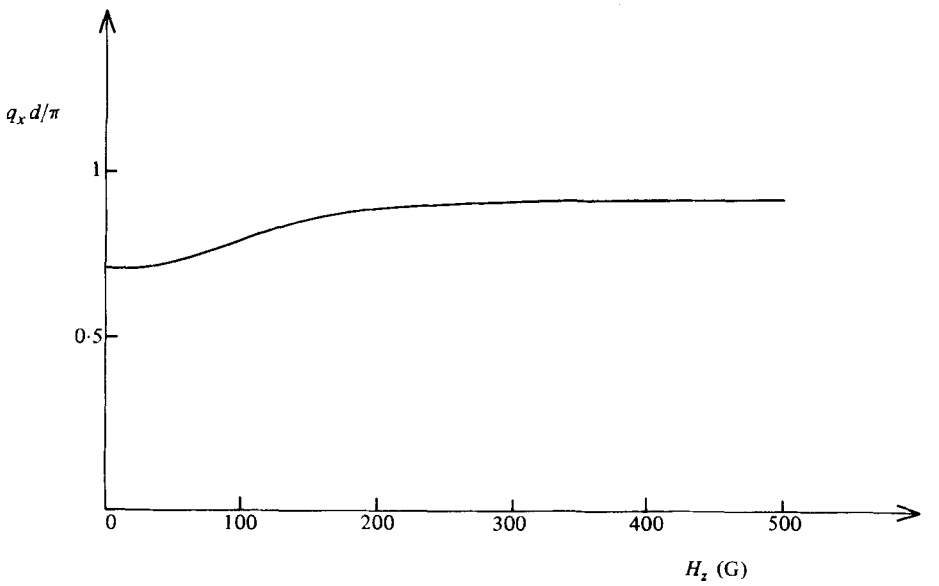

FIGURE 4. Wave vector of the linear solution in the presence of a vertical applied field.

4.1. *Results in the absence of fields*

The critical thresholds for both thicknesses are as follows:

$$\Delta T_c^{\exp} = \begin{cases} -5{\cdot}3^\circ & (d = 1 \text{ mm}), \\ -15{\cdot}5^\circ & (d = 0{\cdot}7 \text{ mm}); \end{cases}$$

$$\Delta T_c^{\text{th}} \approx \begin{cases} -5^\circ & (d = 1 \text{ mm}), \\ -14{\cdot}6^\circ & (d = 0{\cdot}7 \text{ mm}). \end{cases}$$

The theoretical result ΔT_c^{th} was obtained from the two-dimensional analysis of Dubois-Violette (1974) and that of Barratt & Sloan (1976). It is in remarkable agreement with experiments, considering the accuracy on the material parameters for the MBBA used (the source of data is the same as in I).

Besides the expected correspondence as d^{-3} between the ΔT_cs, the geometry of the structure is different for both thicknesses. For the thicker film, it consists of a *square* pattern resulting from crossed rolls. A photograph of the pattern and an analysis of it were given in figure 1 of Pieranski *et al.* (1973) for a film of the same thickness and will not be reproduced here. Parallel rolls are often seen as transient structures in the establishment of the squares. Such a square geometry is compatible with a direct bifurcation by symmetry arguments (Busse 1978).

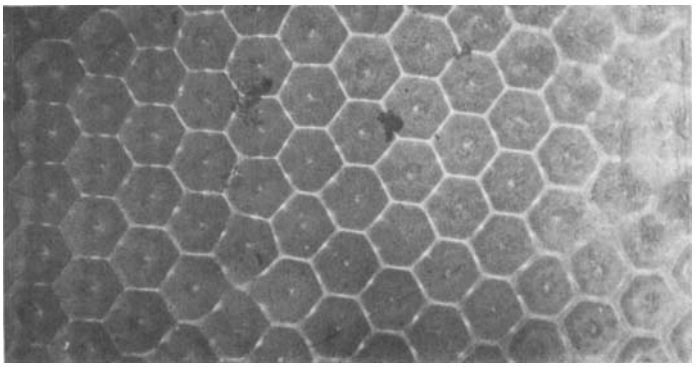

FIGURE 5. Convective pattern at threshold for a large temperature difference $\Delta T_c = 16°$.

On the other hand, for the thinner film ($d = 0{\cdot}7$ mm) the convective pattern at threshold is made of *hexagons*, as shown in figure 5. It is similar to that obtained in the BM thermal instability driven by surface-tension gradients in fluids having an upper free surface (Pearson 1958; Gerbaud 1980). Hexagons were also obtained when non-Boussinesq effects due to the variation of material parameters across the surface layer were important (a recent theoretical work containing references to experiments is Sazontov 1980). Quite generally such hexagons indicate a vertical asymmetry in the system, as shown by Palm, Ellingsen & Gjevik (1967), and discussed in detail by Busse (1978). In nematic MBBA, there is a rapid variation of viscosity coefficients with T, especially near the transition to the isotropic phase: the ratio of the three Miesowicz shear viscosities for MBBA between 37° and 21 °C is $0{\cdot}5 \pm 0{\cdot}05$ (Gahwiller 1973). It is also nearly the value for the twist viscosity γ (Prost & Gasparoux 1971). Similar variations are obtained for the other parameters that enter in the form of ΔT_c. It is thus reasonable to assume that it is this variation that causes the asymmetry of the hexagonal patterns, with hot fluid rising in the central part of the cell (see figure 7).

4.2. *Vertical applied field*

The experimental increase of threshold with the value of the stabilizing field H_z is plotted in figure 6 for the two thicknesses $d = 0{\cdot}7$ and 1 mm. The value of the normalizing field H_0 has been adjusted in each case to fit the simple theoretical quadratic result given by (6); $\Delta T_c(H)$ has been normalized to the above values $\Delta T_c(0)$ in zero field. We note an excellent agreement, beyond the expected range of validity of the formula! In particular, the the value of H_0 is close to that which is deduced

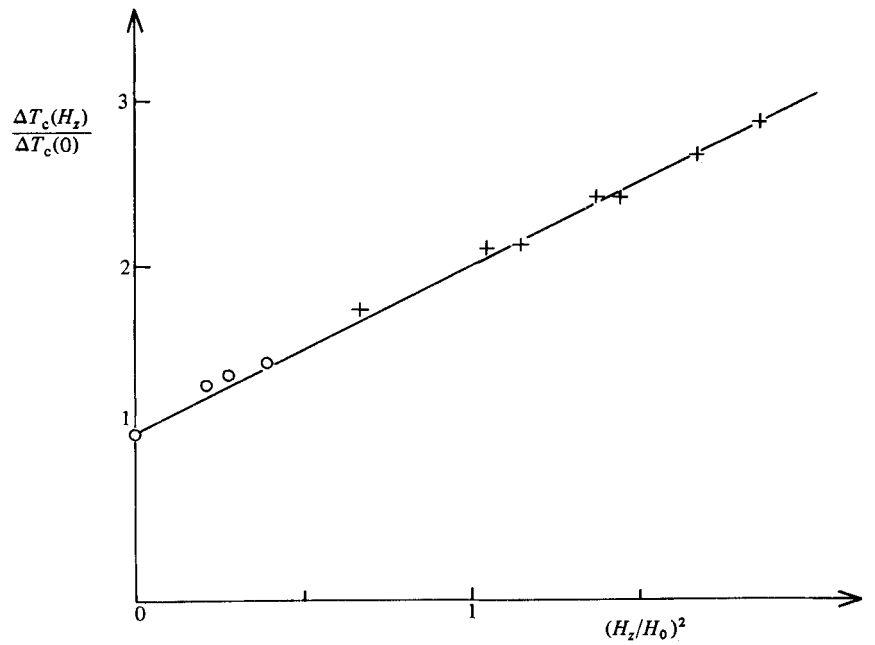

FIGURE 6. Variation of threshold in a vertical applied field for two thicknesses $d = 0{\cdot}7$ mm (○) and 1 mm (+). The values of H_0 have been adjusted to give the best fit with the theoretical straight line (6): $H_0 = 130$ and 85 G.

from the calculated value of H_{c3} ((5), the bend constant) and the correcting factor, given in (7), $H_0^2/H_{c3}^2 \sim 1{\cdot}15$, which takes into account the splay elasticity K_1 in the plane of the film when convection takes place. Experiments on thicker ($d = 5$ mm) films showed that the quadratic behaviour in the field extends to much larger field ratios $h \sim 8$ (I, figure 2).

Several convective geometries are observed at threshold on the thicker film $d = 1$ mm, depending on the value of $\Delta T_c(H)$: as long as $\Delta T_c(H)$ is smaller than 16 °C, the pattern at threshold is made of *squares* as for $H = 0$. There is not much change in the wavelength. This is not inconsistent with the calculation of Gabay (1981) sketched in figure 4 because the field is restricted to a value $H/H_c < 2$ in the experiment.

For larger values of $\Delta T_c(H)$ the pattern at threshold is made of *hexagons*. This result is to be compared with that obtained in §4.1 for a thinner film with $d = 0{\cdot}7$ mm and $H = 0$.

The fact that the value ΔT_c where the change between squares and hexagons takes place is the same in both experiments (despite the different conditions) is a strong indication that the non-Boussinesq character plays an essential role.

For an even larger field (and $\Delta T_c(H)$), the isotropic transition T_{NI} is reached at the upper plate. A typical pattern observed in such conditions is shown in figure 7. The sharp hexagonal lines are the isotherms $T = T_{NI}$ at the level of the upper plate, separating the inner part in the isotropic state (at a temperature $T > T_{NI}$), the outer one still being in the nematic state. The structure grows from normal spots at the centre of the hexagons (showing indeed that warmer fluid climbs in the central region of lower viscosity, as expected from the non-Boussinesq mechanism). It develops up to the point where the hexagonal borders merge into a continuous surface.

For even larger gradients, the nematic phase is separated from the upper plate by

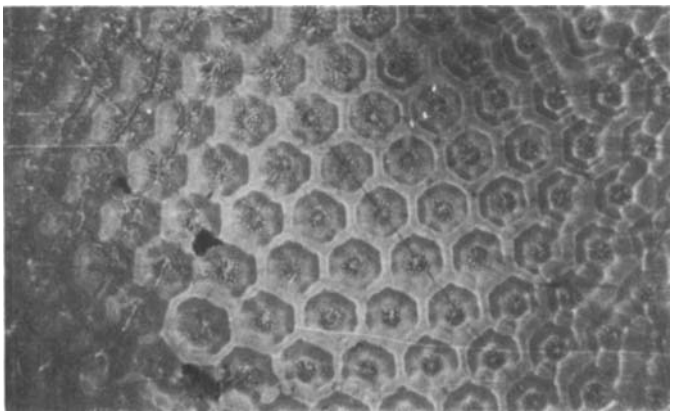

FIGURE 7. Hexagonal convective pattern when the temperature of the upper plate reaches that of the transition to isotropic phase T_{NI}. The inner part of the hexagons is in the isotropic state, and the border lines are the isotherms $T = T_{NI}$.

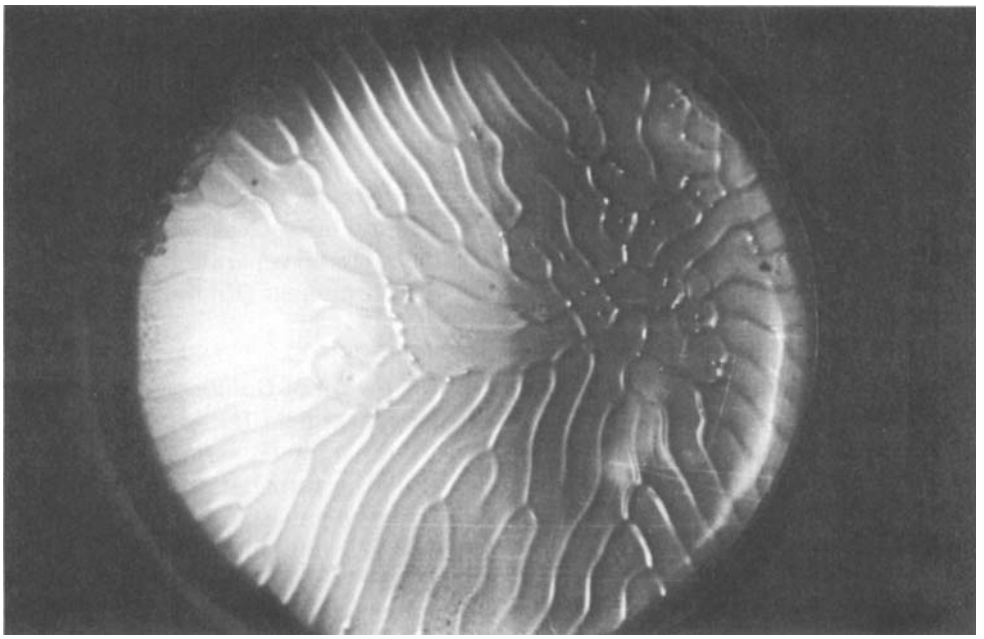

FIGURE 8. Roll structure obtained where an isotropic layer exists below the upper plate at a temperature $T_u \gtrsim T_{NI}$ ($> T_\ell$).

a complete isotropic layer. The static properties of this interface have been studied in particular by Vilanove *et al.* (1974) and involve a radical change in the boundary condition on **n**. Quite surprisingly, we have found that the hexagonal convective pattern is no longer the stable solution at threshold in such a case but is replaced by *rolls*. An observed pattern is shown on figure 8. There is no preferred direction in the plane of the layer, and rolls tend to align normal to the boundaries, as is also found in Rayleigh–Bénard experiments (Storck & Müller 1975). Defects must be created in the central part of the cell in such a circular geometry as observed here. (Let us also note that, in the case of square convection obtained in zero field, the structures also tend to adjust to be perpendicular to the outer walls.)

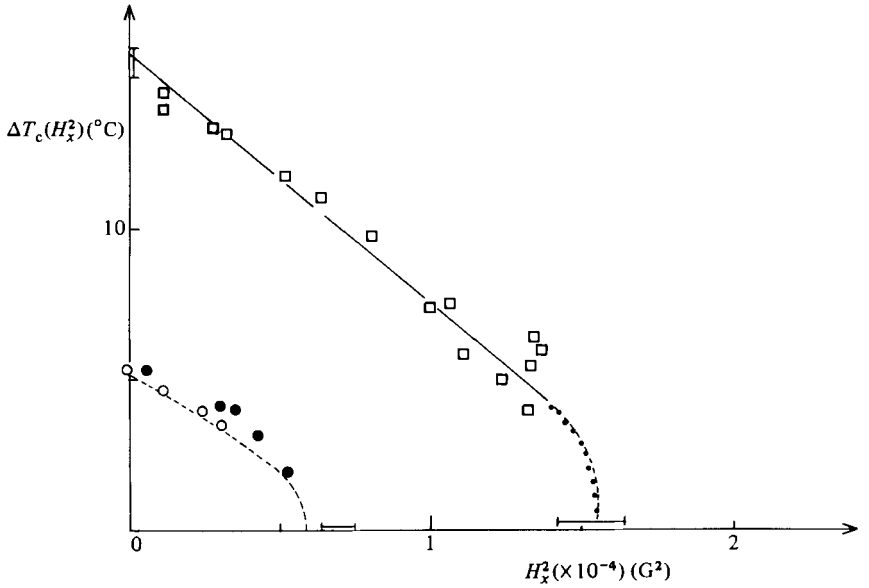

FIGURE 9. Decrease of threshold with horizontal applied field (experimental) for two thicknesses $d = 0{\cdot}7$ mm (□) and 1 mm (two samples ○ and ●). The straight lines give determinations of $H_0 = 136$ and 92 G. The dotted line is the theoretical curve of figure 2. The inaccurately determined thresholds H_{c3} are indicated by a double horizontal line.

The study of convective instabilities with interfaces is a subject that deserves a particular attention because it is a rare experimental case where convection can be produced between two liquid phases of the same material separated by a first-order transition line. This is also a subject of geophysical interest (Fitzjarrald 1981).

4.3. *With horizontal field*

Two kinds of effects are expected from theoretical work of Gabay (1981), as well as our analysis in §3, from the application of a horizontal field H_x.

(i) *The threshold* $\Delta T_c(H_x)$ is reduced below the value for $H_x = 0$ as expected from the analysis leading to (6). This can be understood in terms of the increase of the relaxation time constant t_0 (see(2)) when the destabilizing field H_x increases. The limit $t_0^{-1} = 0$ corresponds to the Freedericksz threshold H_{c3} (for the bend distortion K_3).

(ii) *Geometry.* In zero field, the axes of the square pattern are not defined in this isotropic geometry. For small fields H_x, the orientational degeneracy leading to squares is removed, and rolls perpendicular to the field are preferred: in such a case the distortion of $\mathbf{n}$ takes place in the vertical plane containing $\mathbf{n}$. Rolls not perpendicular to H would lead to additional magnetic energy on $\mathbf{n}(\mathbf{r})$. For $H \lesssim H_{c3}$, the wavelength of rolls must be large, as it should extrapolate to $q_x = 0$ for $H = H_{c3}$, the FZ instability being a homogeneous distortion in the plane of the film.

The experiments fully confirm these predictions.

The threshold values are plotted in figure 9, and show the initial decrease with field predicted by (6). The extrapolation of the straight lines to $\Delta T_c = 0$ lead to values of $H_0 = 136$ G and 92 G for $d = 0{\cdot}7$ and 1 mm, which are consistent with those used in the normalization of figure 5 (130 and 85 G), as expected from theory. However, for larger fields the variation bends over and extrapolates to the value H_{c3} smaller than H_0. The shape is to be compared with the theoretical one of figure 2.

The variation is to be analysed in conjunction with that of the wavevector q_x, given

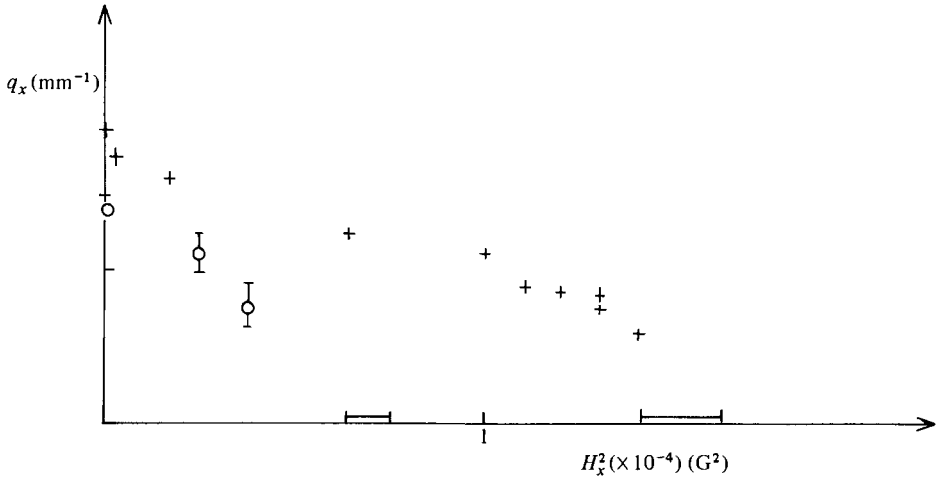

FIGURE 10. Variation of the wave vector $q_z = 2\pi/\lambda_z$ of rolls in the presence of horizontal field for the two thicknesses $d = 1$ mm (○) and 0·7 mm (+). The determination made from photographs is rather inaccurate, but shows qualitatively the continuous decrease of q_x to the homogeneous transition at H_{c3}.

theoretically in figure 3 and obtained from the experimental photographs in figure 10. There is a rather sharp decrease of q_x with field H_x. When H_x approaches H_{c3}, the distortion in the plane of the film becomes negligible with respect to that across the thickness. This reduces the elastic contribution of the theoretical analysis given in (7), which included both bend across the film and splay in the plane in low field, to the simple form (2) (with the single bend constant K_3) next to H_{c3}. The sharpness of the decrease of $\Delta T_c(H_x)$ follows that of q_x. The discussion also indicates that, owing to the different field values that enter in the two regimes of the curve, one cannot use in principle normalized field units to describe the theoretical variation. However, in practice $K_1 \sim K_3$ in many systems, and normalized field axes can then be used.

The behaviour around the critical point $\Delta T_c = 0$, $H = H_{c3}$ indicates an original transition from a dynamic bifurcation (characteristic of a dissipative system like the Rayleigh–Bénard problem) to a bifurcation of thermodynamic nature, i.e. one that can be obtained from the minimization of a free energy, the FZ problem.

The low-field behaviour is helpful in discussing the square → roll transition. Experimentally such a transition is obtained reversibly without any apparent discontinuity of the threshold value as soon as we apply a small field H_x. The linear solution obtained in both cases consists of rolls, and is not expected to show any discontinuous behaviour with the application of fields; only nonlinear terms can tell if the interaction of rolls of different directions lead to squares or not. A particular aspect of convective problems in a degenerate geometry (as for $H_x = 0$) is the so-called 'Brazovski effect'. The initial invariance of the system with respect to rotations about the z-axis causes fluctuations of the periodic structure to induce a first-order transition (inverse bifurcation) (Walgraef, Dewell & Borckmans 1981; Gabay 1981). The thresholds of various convective solutions (rolls, squares, hexagons, ...) can be calculated, but they lie too close to one another to lead to measurable experimental differences so far.

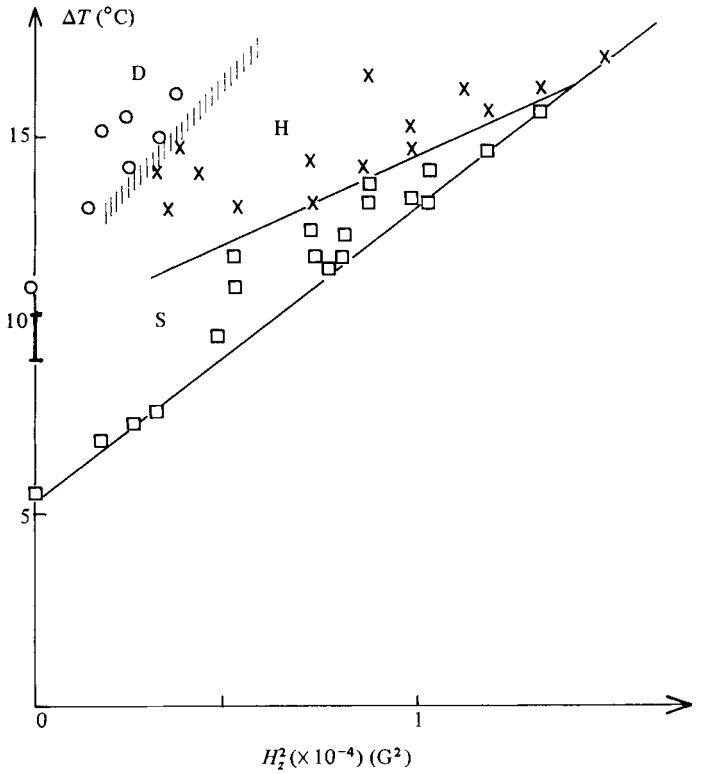

FIGURE 11. Diagram showing the range of stability of squares (S) (□), hexagons (H) (X) and of the disorganized structure (○) for a $d = 1$ mm film in a vertical field H_z. The threshold straight line corresponds to the normalized variation of figure 6. The S–H transition is ill-defined for low fields, where intermediate structures are met. This is not so for large fields.

5. Supercritical behaviour

Owing to the complexity of the theoretical descriptions, we only present, in a schematic form, the development of the instability pattern above threshold. This may be worthwhile in view of the present interest in studying convective geometries: defects (Guazzelli, Guyon & Wesfreid 1981) and phonons (Wesfreid & Croquette 1980).

The phase diagram of figure 11 shows the nature of the structures obtained in the thicker ($d = 1$ mm) cell in stabilizing field H_z. For small-enough fields the linear transition, discussed in §3, leads to a square (S) pattern over a finite range of ΔT. A second transition to hexagons (H) takes place for larger gradients. The border line S–H extrapolates in increasing fields to the critical value $\Delta T_c(H_z) \approx 16°$ that separates the transition to squares from the direct one to hexagons. In the other direction ($H_z \to 0$) the borderline is not so sharply defined, and intermediate structures are observed over a finite range of ΔT. Above the S–H transition, another line is met, which corresponds to the disorganization of the hexagons. Such 'melting' has been observed and analysed in recent work on various systems (Guazzelli & Guyon 1981), and connected with the idea of phase turbulence introduced by Pomeau & Manneville (1979).

The disorganization of the structures has been followed from a slow-speed ciné film, and showed in particular the role of pairs of pentagons and heptagons in the dissociation process by dislocation melting (Toner & Nelson 1981). These effects are

compared and analysed, together with other instabilities where similar disorganization takes place, Pantaloni *et al.* (1980). In the BM structures reported there, an overall rotation of the convective pattern was observed, which was tentatively connected with an Earth Coriolis effect (for a small Rossby number $Ro = v/\Omega d$, v being the convective velocity). In our experiment we have seen no such rotation. However, in the present case, the time constant for the relaxation of the structure is controlled by the diffusivity D_0 acting on an horizontal scale of the cell L. This is much larger than the period of rotation of the Earth. An inequality of opposite sign is obtained in the BM problem, which allows for a movement of the total convective pattern in response to the Coriolis force acting on the convective flow.

We have greatly benefited from several discussions with M. Gabay and from communications of the results of his thèse de doctorat d'Etat; E. Dubois-Violette has largely contributed to theoretical understanding of this problem as well as in the preparation of the manuscript.

The contribution of M. Rachmanidou in the experiments above threshold is acknowledged. We have had discussions with E. Wesfreid, E. Guazzelli and Y. Pomeau on various parts of the work. One of us (J.S.) acknowledges partial support from D. Stiftung Volkswagenwerk.

REFERENCES

Barratt, P. J. & Sloan, D. M. 1976 Thermal instabilities in nematic liquid crystals. *J. Phys.* A: *Math. & Gen.* **9**, 1987.

Busse, F. H. 1978 Non-linear properties of thermal convection. *Rep. Prog. Phys.* **41**, 1929.

Currie, P. K. 1973 The orientation of liquid crystals by temperature gradient. *Rheol. Acta* **12**, 165.

Deuling, H. J. 1978 Elasticity of nematic liquid crystals. *Solid State Phys. Suppl.* **14**, 77.

Dubois-Violette, E. 1971 Instabilités hydrodynamiques d'un nématique soumis à un gradient thermique. *C.r. Acad. Sci. Paris* **275**, 923.

Dubois-Violette, E. 1974 Determination of thermal instability thresholds for homeotropic and planar nematic liquid crystal samples. *Solid State Commun.* **14**, 767.

Dubois-Violette, E., Guyon, E. & Pieranski, P. 1974 Heat convection in a nematic liquid crystal. *Mol. Cryst. Liq. Cryst.* **26**, 193.

Ericksen, J. L. 1962 Hydrostatic theory of liquid crystals. *Arch. Rat. Mech. Anal.* **9**, 371.

Fitzjarrald, D. E. 1981 An experimental investigation of convection in a fluid that exhibits phase change. *J. Fluid Mech.* **102**, 85.

Gabay, M. 1981 Etude de la thermodynamique des verres de spin dans le cadre du champ moyen et de phénomènes critiques dans les cristaux liquides et polymères. Thèse doctorat, Orsay.

Gähwiller, Ch. 1973 Direct determination of the five independent viscosity coefficients of nematic liquid crystals. *Mol. Cryst. Liq. Cryst.* **20**, 301.

Gerbaud, C. 1980 Etude des instabilités convectives dans les phénomènes de Rayleigh–Bénard–Marangoni. Thèse 3ème cycle, Université Aix Marseille I.

Guyon, E. & Pieranski, P. 1973 Convective instabilities in nematic liquid crystals. *Physica* **73**, 184.

Guyon, E., Pieranski, P. & Salan, J. 1979 Overstability and inverted bifurcation in homeotropic nematics heated from below. *J. Fluid Mech.* **93**, 65.

Guazzelli, E. & Guyon, E. 1981 Fusion partielle d'une structure convective bidimensionnelle. *C.R. Acad. Sci. Paris* **292**, 141.

Guazzelli, E., Guyon, E. & Wesfreid, J. E. 1981 Defects in convective structures in an hydrodynamic instability. In *Symmetries and Broken Symmetries in Condensed Matter Physics* (ed. W. Boccara). Paris: IDSET, 456.

LEKKERKERKER, H. N. W. 1977 Oscillatory convective instabilities in nematic liquid crystals. *J. Phys. Lettres* **38**, 277.

LESLIE, F. M. 1968 Some constitutive equations for liquid crystals. *Arch. Rat. Mech. Anal.* **28**, 265.

LIANG, F. F., VIDAL, A. & ACRIVOS, A. 1969 Buoyancy driven convection in cylindrical geometries. *J. Fluid Mech.* **36**, 239.

PALM, E., ELLINGSEN, T. & GJEVIK, B. 1967 On the occurrence of cellular motion in Bénard convection. *J. Fluid Mech.* **30**, 651.

PANTALONI, J., CERISIER, P., BAILLEUX, R. & GERBAUD, C. 1980 Convection de Bénard Marangoni: un pendule de Foucault? *J. Phys. Lettres* **42**, 147.

PEARSON, J. R. A. 1958 On convection cells induced by surface tension. *J. Fluid Mech.* **4**, 489.

PIERANSKI, P., DUBOIS-VIOLETTE, E. & GUYON, E. 1973 Heat convection in liquid crystals heated from above. *Phys. Rev. Lett.* **30**, 736.

POMEAU, Y. & MANNEVILLE, P. 1979 Stability and fluctuations of a spatially periodic convective flow. *J. Phys. Lettres* **40**, 609.

PROST, J. & GASPAROUX, H. 1971 Determination of twist viscosity coefficient in the nematic mesophases. *Phys. Lett.* **36** A, 245.

SAZONTOV, A. 1980 Concerning the selection of convective structure in a fluid with temperature-dependent viscosity. *Isv. Atmos. Oceanic Phys.* **16**, 319.

STORCK, K. & MÜLLER, U. 1975 Convection in boxes: an experimental investigation in vertical cylinders and annuli. *J. Fluid Mech.* **71**, 231.

TONER, J. & NELSON, D. R. 1981 Smectic, cholesteric & Rayleigh Bénard order in two dimensions. *Phys. Rev.* B **23**, 316.

VILANOVE, R., GUYON, E., MITESCU, C. & PIERANSKI, P. 1974 Mesure de la conductivité thermique et détermination de l'orientation des molécules à l'interface nématique isotrope de MBBA. *J. Phys. (Paris)* **35**, 153.

WALGRAEF, D., DEWELL, G. & BORCKMANS, P. 1981 Dissipative structures and broken symmetry. *J. Chem. Phys.* **74**, 755.

WESFREID, J. E. & CROQUETTE, V. 1980 Forced phase diffusion in Rayleigh Bénard convection. *Phys. Rev. Lett.* **45**, 634.